American Mineralogist, Volume 64, pages 874–885, 1979

Geothermometry, geobarometry, and fluid compositions of metamorphosed calc-silicates and pelites, Mica Creek, British Columbia

EDWARD D. GHENT, DAVID B. ROBBINS AND MAVIS Z. STOUT

Department of Geology, University of Calgary
Calgary, Alberta, T2N 1N4 Canada

Abstract

Temperature, pressure, and fluid compositions that prevailed during metamorphism of pelites and calc-silicates from staurolite and kyanite zone rocks of the Mica Creek area, British Columbia, have been estimated from an electron microprobe study of mineral equilibria. Temperatures estimated from Fe–Mg distribution between garnet and biotite range from 570° to 640°C and are generally consistent with temperatures estimated from coexisting calcite and dolomite in nearby rocks. Pressure estimates based on garnet–plagioclase–kyanite–quartz equilibria range systematically from 6 to 8.5 kbar. These estimates are consistent with the geological cross section, which suggests an increase in the depth of structural level exposed from south to north in the study area. Fluid compositions estimated from paragonite–quartz–albite–kyanite equilibria from the metapelites are dominated by H_2O, and fluid compositions estimated for calc-silicates have $X CO_2 > X H_2O$. Calc-silicates formed at carbonate–pelite contacts appear to have equilibrated at temperatures near 610°C and $X CO_2$ near 0.25.

Introduction

The internal consistency of several geothermometers and geobarometers has been tested for staurolite and kyanite zone calc-silicates and pelites from Mica Creek, British Columbia (Fig. 1). These rocks are particularly well suited for such a study, because carbonates and pelites are interlayered and critical mineral assemblages occur over short distances so pressure–temperature variation is likely to be small. In addition, the rocks generally show textural equilibrium, and retrogressive metamorphism is negligible.

We have used the estimated temperatures and pressures in equilibrium constant equations to estimate fH_2O and fCO_2 attending metamorphism of both calc-silicates and pelites. In a separate paper we will report on a stable-isotope study of the calc-silicate rocks.

General geology

The structure and general aspects of the metamorphism at Mica Creek have been discussed by Ghent *et al.* (1977b). The area is underlain primarily by metasedimentary rocks of the Hadrynian (Late Precambrian) Horsethief Creek Group. These rocks have been intensely deformed by at least three phases of folding associated with thrust and subsequent normal faulting. Metamorphic grade ranges from upper garnet zone to lower sillimanite zone, defined by mineral assemblages in pelitic rocks. The following isograds were mapped: (1) first appearance of staurolite with kyanite; (2) disappearance of staurolite; (3) first appearance of abundant migmatite (trondhjemite); (4) first appearance of sillimanite (Fig. 1).

Staurolite disappears in a 200–300 m belt well within the kyanite zone. The first appearance of trondhjemite migmatite very nearly coincides with the staurolite disappearance belt. Sillimanite first appears as fibrolite and is found together with kyanite over a distance of 100–200 m. In cross section the kyanite zone is at least 6 km thick.

High-grade minerals such as sillimanite, kyanite, and staurolite are deformed by phase 3 folds. Migmatite layers are folded and disrupted during phase 3 folding. The metamorphic maximum occurred after or late in phase 2 folding but prior to the bulk of phase 3 deformation. A structural cross section (Ghent *et al.*, 1977b) indicates that rocks at the north end of the study area represent the deepest structural level exposed.

Mineral assemblages and methods of study

Pelite samples from the staurolite and kyanite zones were selected from the Isaac Formation, which

0003–004X/79/0708–0874$02.00

contains abundant aluminous assemblages (Ghent *et al.*, 1977b). The samples were chosen because they contain mineral assemblages for which pressure, temperature, and fluid composition could be estimated. All pelitic samples contain the assemblage quartz–muscovite–biotite–garnet–plagioclase. Two samples (DR187, GM73-11) also contain kyanite as an additional phase, and the following samples contain staurolite plus kyanite: DR135, 158, 194, 219 and GM74-6 and 13. With the exception of minor sericitization of kyanite and very minor alteration of garnet to chlorite, the pelitic rocks show no evidence of retrogressive alteration. Ilmenite and less abundant rutile are the Fe–Ti oxides. Rare sulfides, tourmaline, apatite, and zircon make up the accessory minerals.

Calc-silicate samples from the Cunningham Formation were selected for one or more of the following reasons: (1) the samples contain coexisting calcite and dolomite; (2) the samples contain mineral assemblages whose *P–T* fluid composition history can be modelled by experimental and computed phase equilibria; (3) the samples occur at marble–pelite contacts and contain a large number of coexisting minerals (low-variance assemblages). Mineral assemblages of calc-silicates are reported in Table 1b.

Table 1a. Abbreviations and symbols

ab	albite	K_s	solid activity product
al	almandine	K_D	distribution coefficient
an	anorthite	X_i	mole fraction of component i
bi	biotite	a_i^α	activity of species i in phase α
Ca amph	calcic amphibole	γ_i^α	activity coefficient of species i in phase α
cc	calcite	P_s	pressure on solid phases
chl	chlorite	P_{H_2O}	pressure of H_2O
cpx	clinopyroxene	P_f	pressure on fluid phase
di	diopside	T	temperature
dol	dolomite	f_{H_2O}	fugacity of H_2O
ep	epidote	ΔG_T^P	Gibbs free energy change at P and T
Fe st	Fe staurolite		
ga	garnet		
gr	grossular		
kf	k-feldspar		
ky	kyanite		
ma	margarite		
mgs	magnesite		
mu	muscovite		
pa	paragonite		
phl	phlogopite		
pl	plagioclase		
qz	quartz		
rut	rutile		
sph	sphene		
st	staurolite		
tr	tremolite		
zo	zoisite		

Table 1b. Mineral assemblages in calc-silicates from the Mica Creek area, British Columbia

Sample	cc	dol	qz	bi	ga	ky	tr	di	mu	ep	pl	chl	rut	sph
DR-38	X	X	X	X			X							
DR-39	X	X	X				X							
DR-164	X	X	X				X							
DR-186	X	X	X	X			X				X	X		X
GM74-17	X	X	X				X						X	
GM74-36			X	X	X	X			X	X	X	X		
GM75-4	X		X	X			X	X			X			X
GM77-10	X		X	X			X	X			X			X

For samples GM74-36, GM75-4, and GM77-10 see text for discussion. See Table 1a for abbreviations.

Electron microprobe analyses were made insofar as possible on mineral grains which were in contact or at least within a microscope field of view (<500 μm). In the case of pelite–marble contacts, analyses were taken across the actual contacts over an area of several square mm. We found internally-consistent estimates of P–T–$X\mathrm{CO_2}$ for two separate samples of pelite–marble contacts.

Phase equilibria data used in this study

Experimental and computed phase equilibria used in this study of metamorphosed pelites and calc-silicates are reported as equilibrium constant equations in Table 2.

Fugacity data for H_2O are taken from Burnham *et al.* (1969), and fugacity data for CO_2 are taken from Wall and Burnham (unpublished data). Ideal mixing of H_2O and CO_2 in the fluid phase is assumed, and it is possible that this may lead to significant errors in estimation of low contents of CO_2 in H_2O and *vice versa* (see Holloway, 1977). T–$X\mathrm{CO_2}$ diagrams have been calculated using the computer program XCDFOR of Skippen and Yzerdraat (1970).

For the equilibrium 5 phlogopite + 6 calcite + 24 quartz = 3 tremolite + 5 K-feldspar + $6CO_2$ + $2H_2O$ (Table 2, 5), experimental results have been reported by Hoschek (1973) and Hewitt (1975). These experimental results disagree with one another, but the data of Hoschek are consistent with P–T–$X\mathrm{CO_2}$ estimated from other equilibria (see also Ferry, 1976). Consequently, we have used Hoschek's data in this study.

Hunt and Kerrick (1977) studied the equilibrium calcite + rutile + quartz = sphene + CO_2 (Table 2, 6). They did not report any experimental reversals above 3.45 kbar but obtained a limit on the equilibrium at 5 kbar. Unfortunately the latter point is in

Table 2. Reactions with values of A, B, and C constants for $\log_{10}K = A/T + B + C(P-1)/T$

	Equilibrium	A	B	C	Source of data
1.	pa + qz = ab + ky + H_2O	-4321	8.11	.056	1,2,3
2.	3an + cc + H_2O = 2zo + CO_2	2927	5.03	.346	4
3.	tr + 3cc + qz = 5di + 3CO_2 + 1H_2O	-13832	28.29	.515	4
4.	5mgs + 2cc + 8qz + H_2O = tr + 7CO_2	-33082	63.91	.640	5
5.	5phl + 6cc + 24qz = 3tr + 5kf + 6CO_2 + 2H_2O	-34046	66.28	.792	4
6.	cc + rut + qz = sph + CO_2	-5804	10.49	.119	1,6,7
7.	3dol + kf + H_2O = phl + 3cc + 3CO_2	-18070	31.45	.222	8
8.	3an = gr + 2ky + qz	3272	-8.40	.345	9
9.	6Fe st + 11qz = 4al + 23ky + 3H_2O	-63115	70.94	.598	1,3,10,11
10.	4zo + qz = 5an + gr + 2H_2O	-11675	21.79	-.333	1,3,12,13
11.	2zo + ky + qz = 4an + H_2O	-4027	11.01	-.270	1,3,11,12
12.	2zo + 2ky = ma + 3an	-2850	6.34	.378	1,14
13.	ma + qz = an + ky + H_2O	-9921	18.82	.495	1,3,14

See Table 1a for abbreviations and text for discussion.
1 - calculated by EDG; 2 - Chatterjee, 1971; 3 - Burnham, Holloway and Davis, 1969; 4 - Ferry, 1976; 5 - Rice, 1977; 6 - Hunt and Kerrick, 1977; 7 - Wall and Burnham, unpublished data; 8 - Puhan, 1978; 9 - Ghent, 1976; 10 - Richardson, 1968; 11 - Holdaway, 1971; 12 - Newton, 1966; 13 - Boettcher, 1970; 14 - Chatterjee, 1976.

disagreement with extrapolation from the lower-pressure data. In this study, we derived an equilibrium-constant equation from the lower-pressure data, and we recognize that the calculation at P total $\geq$ 5 kbar carries considerable uncertainty.

Puhan (1978) and Puhan and Johannes (1974) studied the equilibrium 3 dolomite + K-feldspar + H_2O = phlogopite + 3 calcite + 3CO_2 (Table 2, 7) at fluid pressures of 2, 4, and 6 kbar. However, Puhan (1978) calculated the equilibrium curve for a total pressure of 4 kbar, using an equilibrium constant equation derived from the experimental data at 6 kbar, and this calculated curve is considerably different from the experimental curve at 4 kbar. We have averaged the experimental results at 4 and 6 kbar to obtain the equilibrium constant equation reported in Table 2.

For the reaction 3 anorthite + calcite + H_2O = 2 zoisite + CO_2 (Table 2, 2), we have assumed that the free-energy difference between zoisite and iron-free clinozoisite in this pressure–temperature range is negligible.

Garnet–biotite geothermometry

A calibration of Fe–Mg distribution between garnet and biotite, expressed as K_D = (Mg/Fe)ga/(Mg/Fe)bi, with temperature has been made by Thompson (1976), using temperatures based upon other phase equilibria. He pointed out that the effects of cations other than Fe–Mg, *i.e.* Ti in biotite, could cause significant displacement in K_D(Mg–Fe ga–bi) at constant P and T. Goldman and Albee (1977) correlated K_D (Mg–Fe ga–bi) with oxygen-isotope fractionation in coexisting quartz and iron–titanium oxides. They made quantitative estimates of the effects of Ca and Mn contents of garnet and the Fe,Ti and octahedral Al (Al^{VI}) contents of biotite on the correlation between K_D (Mg–Fe ga–bi) and the oxygen-isotope fractionation constant. They presented two equations, one (their equation 6) based on 13 samples for which K_D (Mg–Fe ga–bi) and $^{18}O/^{16}O$ were measured, and a second (their equation 9) based on additional measured K_D (Mg–Fe ga–bi) and *estimated* (calculated) values of $^{18}O/^{16}O$. The temperature calibration of K_D (Mg–Fe ga–bi) was made using experimentally-determined $^{18}O/^{16}O$ fractionation temperatures. Ferry and Spear (1978) have reported experimental data on Mg–Fe exchange between synthetic garnet and biotite. The experiments were done on synthetic annite–phlogopite micas and almandine–pyrope garnets, and these authors suggest that the data can be used on natural biotites and garnets which do not deviate widely from binary solutions.

Electron microprobe data, calculated K_D (Mg–Fe ga–bi), and T (for 5 kbar pressure) for coexisting garnet and biotite from Mica Creek are presented in Table 3. Temperatures have been calculated at 5 kbar using: (1) the calibration of Thompson (1976, p. 431);

Table 3. Garnet and biotite compositions and estimates of temperature

Sample	Mineral	$\ln K_D$	X^{ga}_{Mn}	X^{ga}_{Ca}	X^{bi}_{Fe}	X^{bi}_{Ti}	$X^{bi}_{Al^{vi}}$	T(1)	T(2)	T(3)	T(4)
DR-86	ga core	-1.71	.041	.116				590	530	540	585
	ga rim	-1.78	.044	.117				570	515	525	560
	bi				.529	.049	.134				
DR-130	ga core	-2.07	.090	.084				505	500	475	475
	ga rim	-1.62	.013	.066				610	545	555	615
	bi				.487	.035	.154				
DR-135	ga core	-1.66	.003	.026				605	525	520	600
	ga rim	-1.70	.003	.030				590	515	510	585
	bi				.490	.031	.157				
DR-158	ga core	-2.09	.057	.190				500	495	525	470
	ga rim	-1.80	.005	.083				565	510	525	555
	bi				.463	.029	.155				
DR-187	ga core	-1.91	.015	.198				540	520	580	520
	ga rim	-1.74	.012	.176				580	560	620	575
	bi				.416	.032	.145				
DR-194	ga core	-1.72	.013	.079				585	540	550	580
	ga rim	-1.71	.012	.080				590	540	550	585
	bi				.444	.031	.144				
DR-197	ga core	-1.89	.030	.133				545	520	540	525
	ga rim	-1.78	.023	.102				570	535	550	560
	bi				.435	.032	.142				
DR-219	ga core	-2.30	.021	.165				455	445	460	420
	ga rim	-1.70	.000	.157				605	520	570	590
	bi				.442	.032	.150				
GM73-11	ga core	-1.72	.085	.134				585	580	585	580
	ga int.	-1.74	.081	.135				580	570	575	575
	ga rim	-1.63	.107	.109				620	615	605	615
	bi				.477	.048	.134				
GM73-45	ga core	-1.60	.192	.056				630	590	525	625
	ga int.	-1.61	.192	.056				630	585	525	620
	ga rim	-1.83	.232	.054				570	560	485	545
	bi				.678	.052	.133				
GM73-102	ga core	-1.26	.033	.104				740	660	725	775
	ga rim	-1.56	.078	.097				640	605	615	640
	bi				.500	.043	.163				
GM74-6	ga core	-2.10	.034	.134				510	480	480	470
	ga int.	-2.13	.031	.144				500	475	475	460
	ga rim	-1.56	.022	.104				640	585	605	640
	bi				.434	.041	.116				
GM74-13	ga core	-2.42	.034	.203				445	410	430	395
	ga int.	-2.06	.011	.139				515	450	470	480
	ga rim	-1.64	.009	.080				620	515	535	610
	bi				.548	.043	.168				
GM74-36	ga core	-1.81	.095	.134				575	595	605	550
	ga rim	-1.66	.103	.160				615	655	690	600
	bi				.410	.034	.150				
GM77-10	ga core	-1.74	.060	.123				590	565	590	575
	ga rim	-1.85	.085	.115				565	555	540	540
	bi				.453	.045	.118				

T(1) calculated from Thompson (1976) at 5 kbar, T(2) calculated from Goldman and Albee (1977) eqn. 6, T(3) calculated from Goldman and Albee (1977) eqn. 9, T(4) calculated from Ferry and Spear (1978), For other symbols and abbreviations see text and Table 1a.

(2) equations 6 and 9 of Goldman and Albee (1977); and (3) the calibration of Ferry and Spear (1978).

The garnet–biotite geothermometer has a resolution of approximately ±30°C (2 standard deviations) which corresponds to the error in temperature when errors of ±2 percent relative in FeO and MgO analyses are propagated through the Thompson and Ferry–Spear equations at 5 kbar pressure (see also Ferry and Spear, 1978, p. 117).

Garnets are typically zoned, but biotites are relatively homogeneous. Tracy *et al.* (1976), in a study of garnets and biotites from central Massachusetts, report garnet interior–biotite temperatures (Thompson calibration) that are higher than those estimated for garnet rims and biotite. They argued that garnet rim compositions have been modified by lower-temperature reactions. Our results (Table 3) suggest that for many garnet–biotite pairs, garnet rim–biotite temperatures are *significantly higher* than those estimated from garnet interiors and biotites. These data suggest that many of these staurolite- and kyanite-zone garnet rims and adjacent biotites retain the high-temperature Mg–Fe fractionations. Ghent (1975) reported several analyses of garnet rims and biotites from the staurolite- and kyanite-zone rocks of the Esplanade Range, British Columbia, that yield estimated temperatures which are significantly higher than those from garnet interiors and biotites.

Most of the estimated temperatures from garnet rim–biotite pairs within a single probe section agree to better than 15°C. One sample (GM74-6), however, contains domains, several mm apart, which show significantly different garnet rim–biotite temperatures. For one domain, $\ln K_D$ (Mg–Fe ga) is −1.56 (640°C, Thompson calibration) and for the second domain, it is −1.21 (760°C). The garnets from the two domains have similar Mg/Fe ratios, but the biotites have significantly different Mg/Fe ratios. Other elements, *e.g.* Ti in biotite, are present in similar concentrations in both domains. The proportion of garnet relative to biotite is large, but garnet interior–biotite temperatures are *lower* than garnet rim–biotite temperatures, suggesting that retrogression is not the cause of the disagreement in estimated temperature (see Tracy *et al.*, 1976, p. 768). Because the lower garnet rim–biotite temperature estimate (640°C) is reasonably close to two nearby garnet rim–biotite temperature estimates (620°C and 615°C, Table 13, Fig. 1) we have used this value in subsequent discussions. It is possible that the higher value of $\ln K_D$ (−1.21) does not represent equilibrium fractionation between garnet and biotite in that domain.

Agreement between garnet rim–biotite temperatures calculated from the Thompson calibration and the Ferry and Spear calibration is good (Table 3), but there is poor agreement between these calibrations and the Goldman and Albee calibration, particularly at higher temperatures. Goldman and Albee suggested that this may be due to inaccuracies in the experimental calibration of oxygen-isotope fractionation at higher temperatures. We would argue that these differences could also be due to $^{18}O/^{16}O$ exchange being frozen in at lower temperatures than Mg–Fe exchange.

Garnet–plagioclase–aluminum silicate–quartz equilibria

The solids activity product, $K_S = (X^{gr}_{ga})^3/(X^{pl}_{an})^3$ in the assemblage garnet–plagioclase–Al_2SiO_5–quartz,

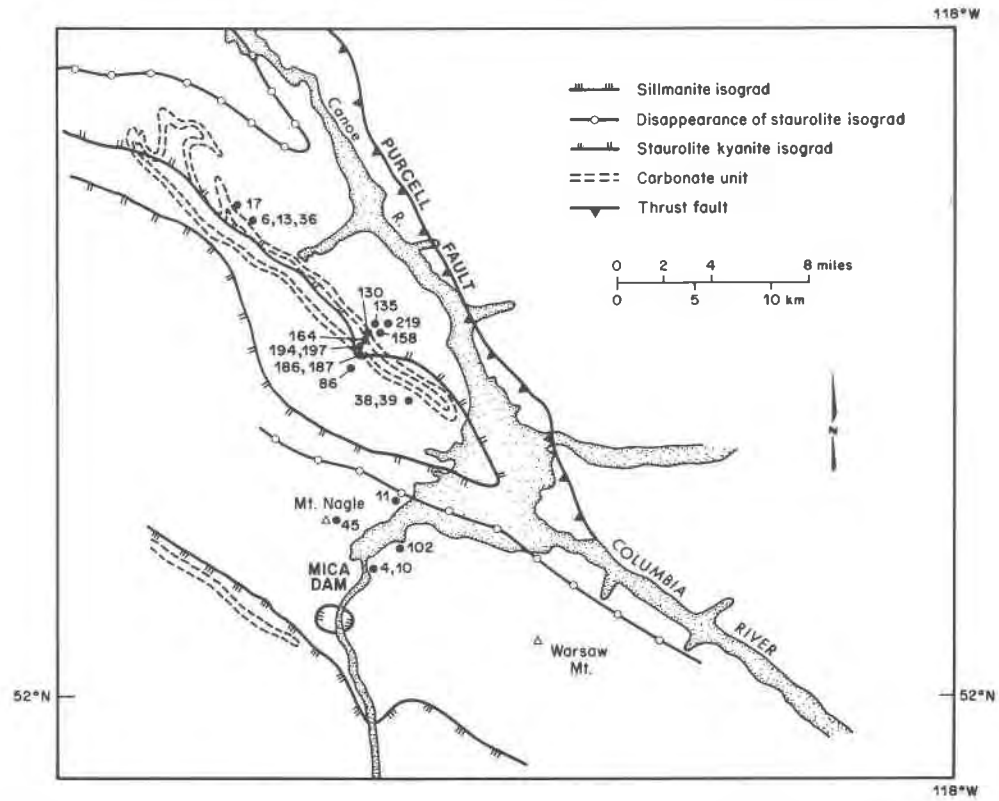

Fig. 1. Simplified geologic map of the Mica Creek area, British Columbia, showing location of samples referred to in this paper. For a more detailed map see Ghent *et al.*, 1977b, p. 13. Appearance of migmatite line is omitted for clarity.

varies systematically as a function of the Al_2SiO_5 polymorph present, and this solids activity product can be used as a relative indicator of metamorphic pressures and temperatures (Ghent, 1975, 1976; Woodsworth, 1977; Ghent *et al.*, 1977a; Blümel and Schreyer, 1977).

The *P–T* calibration of this equilibrium uses the end-member reaction

$$3 \text{ anorthite} = \text{grossular} + 2\ Al_2SiO_5 + \text{quartz} \quad (8)$$

and requires accurate activity–composition data as a function of P and T for the anorthite component in plagioclase and the grossular component in garnet. Experimental data on activities of anorthite at low molar concentrations and $T < 700°C$, $P > 2$ kbar are lacking (Orville, 1972), and there are only limited data on grossular–almandine solutions (Hensen *et al.*, 1975; Newton *et al.*, 1977).

In the absence of experimental data we propose the use of an empirical activity coefficient product (K_γ). For reaction (8) we have

$$\Delta G_T^P = 0 = \frac{-3272}{T} + 8.3969 - \frac{3448(P-1)}{T} + \log K_s + \log K_\gamma \quad (8a)$$

(Ghent, 1976), where kyanite is the Al_2SiO_5 polymorph and $K_\gamma = (\gamma_{gr}^{ga})^3/(\gamma_{an}^{pl})^3$.

We propose that a reasonable estimate of K_γ can be made as follows (see also Ghent, 1976): (1) samples are selected which straddle a kyanite–sillimanite isograd and values of K_s for these samples are obtained; (2) using these values of K_s and Holdaway's (1971) kyanite–sillimanite curve, we solve for log K_γ at several P,T points on the kyanite–sillimanite curve. This calculation assumes that the experimental kyanite–sillimanite curve is a good *P–T* model for the kyanite–sillimanite isograd. An average value for $\log K_s$ is $-2.0 \pm .2$ (Ghent, 1976; Pigage, 1976), and this leads to an average $\log K_\gamma$ of -0.4 (see Fig. 2 for a graphical representation of the calculation). Since the curves for reaction (8) are not precisely parallel to the kyanite–sillimanite curve, it is necessary to average the values of $\log K_\gamma$. This average value of $\log K_s$ (-0.4) can be added to equation (8a) as an empirical correction to the values of γ_{gr}^{ga} and γ_{an}^{pl}. When more accurate experimental data are available, these can be used in place of the empirical activity coefficient ratio.

The concentration of grossular in garnet deter-

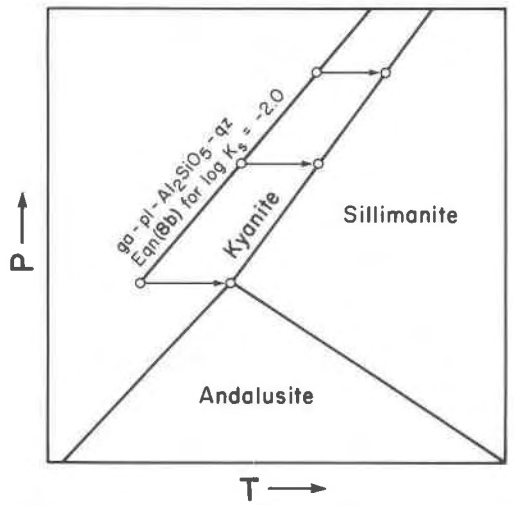

Fig. 2. Pressure–temperature diagram illustrating the method of estimating log K_γ for reaction (8).

mined by electron microprobe analysis is usually expressed as the atomic ratio of Ca/(Ca + Mg + Fe + Mn), where total iron is treated as ferrous. This leads to a *maximum* estimate of grossular component and to a *maximum* estimate of P at constant T and a_{an}^{pl} (Ghent *et al.*, 1977a). We have estimated the ferric-iron content of garnet by normalizing atomic Ca + Mg + Fe + Mn + Al to 5 cations. The number of ferric-iron cations is then combined with calcium cations in the ratio 2:3 to make andradite.

This reduction in the estimated grossular component leads to a reduction in the estimated pressure, at constant T, of 170 to 840 bars. In most cases, however, the reduction is less than 300 bars.

The garnet–plagioclase–Al_2SiO_5–quartz geobarometer has a resolution of approximately ±1.6 kbar (2 standard deviations). This estimated resolution is the pooled estimate of standard deviation which results from combining a standard deviation of ±15°C in T from the garnet–biotite geothermometry and an error of ±1 percent grossular and ±1 percent anorthite in K_8.

Values of logK_8 for reaction (8) and estimated pressures using garnet–biotite temperatures are presented in Table 4.

Mineral equilibria in the system CaO–Al_2O_3–SiO_2–H_2O

Light gray-green fine-grained schists, interlayered on a scale of a few meters with pelitic schists, contain quartz–muscovite–biotite–garnet–plagioclase–kyanite–epidote (GM74-36, Table 1b). These minerals occur in the same hand specimen, but garnet and kyanite do not occur in the same electron microprobe section (a disc of 2.54 cm diameter).

Temperature estimated from garnet rim–biotite geothermometry in sample GM74-36 is 615°C (Table 3), which is in reasonable agreement with temperatures estimated from two nearby pelitic samples, 640°C and 620°C (Table 3, Thompson calibration, and Fig. 1). Using the calibrations of Goldman and Albee, however, produces a T difference of 140°C to 155°C.

Using a T of 615°C, the metamorphic pressure estimated from garnet–plagioclase–kyanite–quartz (GM74-36) is 6 kbar. Nearby pelitic samples yield pressure estimates of 8.2–8.5 kbar (Table 4), which are significantly higher. Possible reasons for this disagreement are discussed below.

The minerals epidote, plagioclase, and kyanite participate in equilibria shown in Figure 3 and given in Table 2. When the solids are modified for solid solution (Appendix; Table 9), P_s–T conditions should lie along a curve such as 11 (Fig. 3), for $PH_2O = P_s$. Although margarite is not present in the assemblage, the *lack* of margarite sets limits on the P_s–T conditions (curve 12, Fig. 3). If the activity of margarite were less than one, the curve would move to higher pressures at constant temperature. For the assemblage epidote–plagioclase–kyanite–quartz, the *minimum* P_s at 600°C is near 7 kbar.

There are several possible ways to explain the disagreement between these pressure estimates. Errors in the experimental phase equilibria and inadequacies

Table 4. Activity products for coexisting garnet and plagioclase and estimates of pressure

Sample	log Ks(8)	T(1)	P(1)	T(2)	P(2)
DR-158	-1.35	570	6.7	510	5.6
DR-187	-1.50	580	6.6	560	6.2
DR-194	-1.63	590	6.4	540	5.5
DR-197	-1.26	570	7.0	535	6.3
DR-219	-1.63	605	6.7	520	5.2
GM73-11	-1.25	620	8.0	615	7.9
GM73-102	-2.18	640	5.9	605	5.3
GM74-6	-1.31	640	8.2	605	7.5
GM74-13	-1.06	620	8.5	515	6.4
GM74-36	-1.98	615	6.0	655	6.7

log Ks(8) = 3 log X_{gr}^{ga} - 3 log X_{an}^{pl}

T(1) Temperature for ga rim-biotite calculated from Thompson (1976) at 5 kbar

P(1) Pressure calculated at T(1) using log Kγ = -0.4

T(2) Temperature for ga rim-biotite calculated from Goldman and Albee (1977) eqn. 6.

P(2) Pressure calculated at T(2) using log Kγ = -0.4.

in the activity models for the crystalline solution could contribute to this disagreement. The fact that kyanite and garnet do not occur in the same microprobe section suggests the possibility that garnet–plagioclase–quartz assemblages were not saturated with kyanite, *i.e.* $aAl_2SiO_5 < 1$. If this interpretation is correct, curve 8 (Fig. 3) gives the *minimum* pressure at a given temperature and is then consistent with other estimates.

Inspection of Figure 3 reveals that epidote–kyanite–quartz–plagioclase (curve 11) could not be in equilibrium at the same PH_2O as epidote–quartz–plagioclase–garnet (curve 10). A calculation of fH_2O at 615°C and P_s = 8 kbar suggests that epidote–kyanite–quartz–plagioclase equilibrated at higher fH_2O than epidote–quartz–plagioclase–garnet. If these assemblages are indeed in equilibrium at the same P_s and T, a gradient in fH_2O on the order of several kbar is suggested, and the fluids would be rich in H_2O ($XH_2O > 0.6$).

Fugacity of H_2O in metamorphosed pelites

The equilibrium, paragonite + quartz = albite + kyanite + H_2O (1, Table 2), can be used to estimate fH_2O for the assemblage K–Na muscovite + quartz + plagioclase + kyanite for a given P_s and T(Ghent, 1975, p. 1659).

The activity of paragonite component [$NaAl_2Si_3O_{10}(OH)_2$ = Pa] in muscovite crystalline solution is $(X\text{Na})(X\text{Al}^{\text{VI}})^2(\gamma^{\text{mu}}_{\text{pa}})$ (see Ferry, 1976, p. 141). In this expression, substitution for Al on octahedral sites (Al^{VI}) is considered to be coupled with substitution for Al by Si on tetrahedral sites. The activity coefficient for paragonite component in muscovite crystalline solution ($\gamma^{\text{mu}}_{\text{pa}}$) for each sample is calculated from the experimental data on the binary muscovite–paragonite system [equation (28) in Eugster *et al.*, 1972, p. 175 and equation (80a) of Thompson, 1967, p. 353], electron microprobe analyses of coexisting muscovite and plagioclase, and temperature and pressure estimates from Table 4. The activity of albite component in plagioclase ($a^{\text{pl}}_{\text{ab}}$) in these samples is taken as $X^{\text{pl}}_{\text{ab}}$ because for the composition range shown by Mica Creek plagioclase $\gamma^{\text{pl}}_{\text{ab}}$ is estimated to be 1.0 (Orville, 1972).

The equilibrium constant equation (1, Table 2) is derived from experimental data on the pure phases (Chatterjee, 1972). In these experiments, albite has a disordered structure. Pigage (1976) estimated the PH_2O–T curve for equilibrium (1), using low albite instead of high albite. He estimated the P–T curve for the reaction low albite = high albite from the thermochemical data of Robie and Waldbaum (1968). Orville (1974) has presented arguments that low albite cannot show more solid solution than An_2 and that the disordered albite structure can dissolve more anorthite than An_2. The transformation low albite to high albite is considered to take place at 575±50°C. For these reasons, we have used disordered pure albite as the standard state in our calculations of fH_2O.

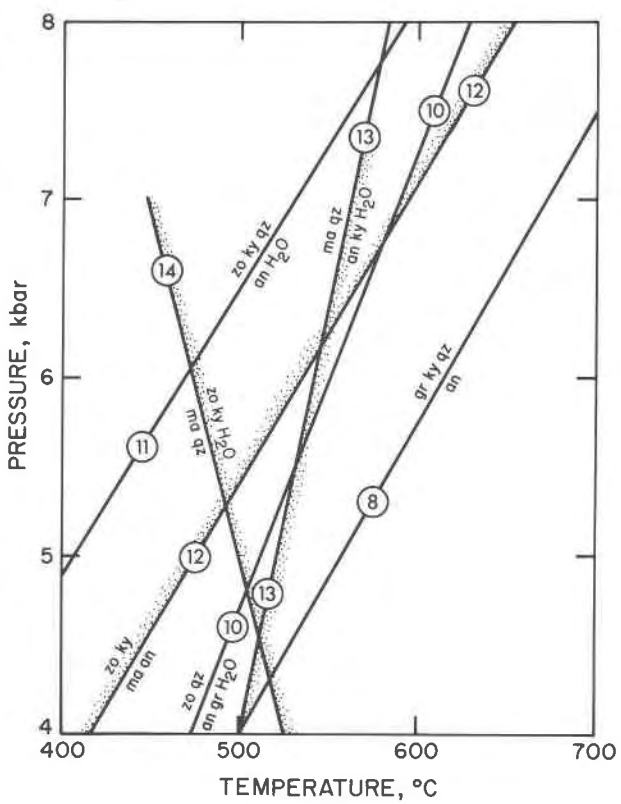

Fig. 3. Pressure–temperature diagram for reactions in the CaO–Al_2O_3–SiO_2–H_2O system. Reactions have been modified for solid solution. Stable assemblages of phases in reactions indicated by stippling on stable side of reaction curve. For example, zo + ky is stable in reaction (12).

Values of fH_2O have been calculated using two sets of pressure–temperature estimates (Table 4), and we report the results as a mole fraction of H_2O (XH_2O) in the fluid, where XH_2O = fugacity of H_2O estimated for the equilibrium divided by fugacity of pure H_2O at the same P and T ($XH_2O = fH_2O/f^*H_2O$). Either set of mole fractions of H_2O (Table 5) should be regarded as being lower than the true values. Substitution of $(\text{Mg,Fe})^{\text{VI}}(\text{Si})^{\text{IV}} = (\text{Al}^{\text{VI}})(\text{Al}^{\text{IV}})$ ("phengite" substitution) is treated as a dilutant in the paragonite–muscovite crystalline solutions. Since the "phengite" substitution is treated as ideal, this treatment results in a maximum reduction in the activity

Table 5. Activity products for paragonite–albite and staurolite–garnet equilibria and estimates of X_{H_2O}

Sample	log $K_s(1)$	$X_{H_2O}(1)$	$X_{H_2O}(2)$	$X^{st}_{Fe\ st}$	X^{ga}_{al}	log K_s (Fe st–al)
DR-158	-0.41	0.64	0.42	0.79	0.77	0.14
DR-187	-0.66	0.48	0.43	-	-	-
DR-194	-0.52	0.61	0.44	0.80	0.74	0.44
DR-197	-0.54	0.47	0.37	0.81	0.72	0.62
DR-219	-0.60	0.77	0.44	0.81	0.75	0.42
GM74-6	-0.86	0.43	0.36	0.77	0.68	0.65
GM74-13	-0.66	0.47	0.24	0.80	0.78	0.13

log $K_s(1)$ is log a^{mu}_{pa} - log a^{pl}_{ab}. See text for explanation

$X_{H_2O}(1)$ calculated from P_1T_1 (Table 4), log $K_s(1)$ and eqn. 1, Table 2.

$X_{H_2O}(2)$ calculated from P_2T_2 (Table 4), log $K_s(1)$ and eqn. 1, Table 2.

of paragonite component in the crystalline solution. Using the equilibrium constant, $K_{(1)} = [(fH_2O)(a^{pl}_{ab})]/(a^{mu}_{pa})$, if the estimate of a^{mu}_{pa} is too low, the result is *too low* an estimate of fH_2O. Experiments on the stability of celadonite (Wise and Eugster, 1964) and phengite (Velde, 1965) suggest that phengite substitution in muscovite should not increase the P_s–PH_2O–T stability field of muscovite–phengite crystalline solution relative to pure muscovite. The treatment of phengite substitution that we have used, however, results in an increase in the stability field of muscovite–phengite crystalline solution and consequently *too low* an estimate of fH_2O at a given P_s and T.

Staurolite–quartz–garnet–kyanite equilibria

The assemblage staurolite–quartz–garnet–kyanite occurs in several samples, suggesting that the equilibrium

$$6HFe_2Al_9Si_4O_{24} + 11SiO_2 = 4Fe_3Al_2Si_3O_{12} + 23Al_2SiO_5 + 3H_2O \quad (9)$$

(Richardson, 1968; Ganguly, 1972) may be applied to estimate P_s, T, and fH_2O conditions of metamorphism. Using the experimental data of Richardson (1968) and the computations of Ganguly (1972) for equilibrium (9) with sillimanite and using the experimental data of Holdaway (1971) for the kyanite–sillimanite equilibrium we obtain the following equilibrium constant equation:

$$3 \log fH_2O = -63115/T + 70.94 + 0.598(P-1)/T \quad (9a)$$

Because there are only 2 reversed P–T brackets, there is a large uncertainty in the A and B constants.

Electron microprobe analyses of staurolite indicate very small amounts of Ti, Zn, and Mn in solid solution and a fairly narrow range of Ti content. The cationic substitution in staurolite is complex (Smith, 1968; Griffen and Ribbe, 1973), and it is difficult to arrive at a simple solid-solution model. We have set $a^{st}_{Fe\ st} = (XFe)^2$, assuming independent mixing on two sites only (see, for example, Pigage, 1976, and Appendix). For the activity of almandine component in garnet, we set $a^{ga}_{al} = (XFe)^3$ and assume negligible ferric iron in the 6-fold site. Using estimated garnet–biotite temperatures and estimated garnet–plagioclase–kyanite–quartz pressures, we can use the above solution models and electron probe analyses to estimate fH_2O from equation (9a). The fugacities of H_2O when converted to mole fractions suggest XH_2O in the range 4–8 $\times 10^{-4}$. Using the lowest positive P–T slope consistent with the experimental data, the values of XH_2O are increased to about 0.02. These results are in severe disagreement with XH_2O estimated from the same samples by paragonite–quartz–albite–kyanite equilibria. We suggest that this discrepancy is largely due to the experimental location of equilibrium (9) in P_S—P_{H_2O}—T space. Similar discrepancies between staurolite equilibria and other equilibria in pelitic rocks have been noted by Thompson (1976) and Carmichael (1978).

Calcite–dolomite geothermometry

The magnesium content of calcite coexisting with dolomite has been shown experimentally to be a sensitive function of temperature and a less sensitive function of pressure (Goldsmith and Newton, 1969). One of the difficulties in the application of this geothermometer to natural calcite–dolomite pairs is that high-Mg calcite can exsolve dolomite upon cooling, thus making difficult the reconstruction of the original single-phase composition. In our study, we have taken averages of several grains per sample using both a defocussed beam and scans across individual grains. In Table 6, we report the highest average Mg analyses of individual grains in a sample.

The results from four samples range from 580 to 600°C at 5 kbar and about 10°C lower at 7 kbar (Table 6). The calcite and dolomite also contain small amounts of siderite in solid solution. Using the equations set forth in Bickle and Powell (1977), average temperature estimates based on both calcite and dolomite are increased by approximately 5–10°C at 5 kbar. These temperatures are in reasonable agreement with garnet–biotite temperatures estimated from Thompson's (1976) calibration (Table 3).

Table 6. Estimates of temperature based on magnesium contents of calcite coexisting with dolomite

Sample	Magnesite	Siderite	T(5 kbar)	T(7 kbar)
DR-38	6.6	0.3	580	570
DR-39	6.4	0.6	570	565
DR-164	6.8	0.5	585	580
DR-187	7.2	0.7	600	590

Magnesite and siderite contents reported in molecular per cent.

Table 7. Estimates of fluid composition based on dolomite-quartz-tremolite-calcite equilibria

Sample	T	P	X_{CO_2}
DR-38	580 ± 10	6 ± .5	0.81 ± 0.11
DR-39	580 ± 10	6 ± .5	0.82 ± 0.11
DR-164	580 ± 10	6.5 ± .5	0.76 ± 0.11
DR-186	590 ± 20	6.5 ± .5	0.81 ± 0.15
GM74-17	600 ± 20	7.5 ± 1.0	0.78 ± 0.21

See text for discussion of pressure and temperature estimates.

Dolomite–calcite–quartz–tremolite equilibria

Five samples contain the assemblage dolomite–calcite–quartz–tremolite (Table 1, Fig. 1). Following Skippen (1975), these phases participate in the following equilibrium: 5 magnesite + 2 calcite + 8 quartz = tremolite + $7CO_2$ + H_2O (Table 2, 4).

Temperatures attending metamorphism of these samples can be estimated from dolomite–calcite equilibria (Table 6) and garnet–biotite equilibria in nearby pelitic samples (Table 3). Pressures attending metamorphism can be estimated from garnet–plagioclase–kyanite–quartz equilibria in nearby pelitic samples (Table 4).

Using electron microprobe analyses of tremolite, we have calculated activities of tremolite in Ca-amphibole (Table 8; Appendix). The expression for activities of $CaCO_3$ and $MgCO_3$ are taken from Gordon and Greenwood (1970). Using these solid-species activities and equation (4), Table 2, we have calculated a set of isobaric T–XCO_2 curves for each sample. In several cases (*e.g.* GM74-17), the highest temperature estimates for nearby garnet–biotite assemblages are near the maximum stability limit of the tremolite–calcite–quartz assemblage at 5 kbar, and we have used the maximum temperature consistent with the stability of the assemblage. Fluid composition estimates vary from XCO_2 = 0.76 to 0.81 with an uncertainty on the order of 0.2 XCO_2 (Table 7). These estimates are consistent with internal control of fluid composition by the mineral assemblage.

Carbonate–pelite contacts

Contacts between pelites and carbonate rocks are the loci of metamorphic reactions which produce low-variance mineral assemblages. Such contacts have been studied in other areas to elucidate the effects of gradients in the activities of volatile components and mass transfer of cation or anion species (*e.g.*, Vidale and Hewitt, 1973; Thompson, 1975a,b). In the Mica Creek area we have focussed our attention on estimation of temperature and fluid composition based on the calc-silicate assemblages developed in the reaction zones between pelites and carbonates. Two samples (GM75-4 and GM77-10, Fig. 1) have been selected for detailed study. Mineral assemblages for these samples are given in Table 2, and the detailed assemblages and dimensions of the zones are given in Table 8.

The following equilibria can be applied to these assemblages.

(2) 3an + cc + H_2O = 2zo + CO_2
(3) tr + 3cc + qz = 5di + $3CO_2$ + H_2O
(5) 5phl + 6cc + 24qz = 3tr + 5Kf + $6CO_2$ + $2H_2O$
(6) cc + rut + qz = sph + CO_2
(7) 3dol + Kf + H_2O = phl + 3cc + $3CO_2$

Activities for components participating in equilibria (2), (3), (5), (6), and (7) have been calculated from mineral compositions and the activity–composition expressions given in the Appendix. These activities are listed in Table 9. Equilibria (2) and (3) intersect on isobaric T–XCO_2 diagrams; the other equilibria can be used to set limits on isobaric T–XCO_2 diagrams.

A pressure estimate for a pelitic assemblage 2.4 km away (GM73-102) is between 5 and 6 kbar (Table 4). Using $P_f = P_s$ = 5.5±0.5 kbar and equilibria (2) and

Table 8. Mineral assemblages at carbonate–pelite contacts, Mica Creek, British Columbia

Zone	Sample GM77-10	Sample GM75-4
carbonate	cc-qz-di-ep	cc-qz-di-ep
reaction zone 1	di-ep-pl-qz-sph-cc (3-4 mm thick)	di-ep-pl-qz-cc (4-5 mm thick)
reaction zone 2	qz-Ca amph-ep-di-sph-pl (1-2 mm thick)	qz-Ca amph-ep-di-sph-pl (1-2 mm thick)
reaction zone 3	qz-Ca amph-pl-sph (4-5 mm thick)	Ca amph-bi-qz-pl-sph (2 mm thick)
pelite	qz-pl-bi-ga-cp	qz-pl-bi-sph

For abbreviations of minerals see Table 1a.

Table 9. Activities of species in Mica Creek calc-silicates

Sample	an	zo	tr	di	phl
GM75-4	0.96	0.84	0.015	0.54	0.092
GM77-10	0.92	0.75	0.048	0.57	0.070
GM74-36	0.68	0.41			
DR-38			0.765		
DR-39			0.799		
DR-164			0.780		
DR-186			0.626		
GM74-17			0.279		

For method of calculation of activities of species. For abbreviations, see Table 1a.

(3), we estimate the following T–$X\mathrm{CO_2}$ conditions:

GM75-4, $T = 610\pm15°C$, $X\mathrm{CO_2} = 0.23\pm0.04$

GM77-10, $T = 610\pm15°C$, $X\mathrm{CO_2} = 0.27\pm0.04$

The uncertainties quoted are the values calculated at the extreme pressure limits. These estimates are within the T–$X\mathrm{CO_2}$ limits set by equilibria (5), (6), and (7).

Discussion and conclusions

Estimates of pressures and temperatures attending metamorphism are summarized in Figure 4. As discussed previously, garnet–biotite temperature estimates (Thompson and Ferry–Spear calibrations) are in reasonable agreement with calcite–dolomite temperature estimates from nearby carbonate samples. Two temperature estimates from calc-silicate equilibria differ from a single garnet–biotite temperature by 50°C but are within 30°C of garnet–biotite temperatures in nearby pelitic rocks.

Pressure estimates range from near 6 kbar in the south part of the area (using Thompson and Ferry–Spear temperature estimates) to 8.5 kbar in the north part of the area. There are some reversals in the regional trend, but the pressure estimates from geobarometry are generally consistent with the structural cross section through the south-plunging structures, that is, the depth of structural level exposed increases from south to north. The higher pressure estimates from the north part of the area are also supported by epidote–kyanite–plagioclase and epidote–quartz–garnet–plagioclase equilibria (Fig. 3). The higher pressure estimates are at least 1 kbar higher than the upper pressure limits on bathozone 5 estimated by Carmichael (1978) (Fig. 4).

Fugacities of H_2O estimated from mineral equilibria are, from highest to lowest: pelite–carbonate reaction zones, pelitic rocks (paragonite–quartz–albite–kyanite equilibria), and marbles (dolomite–quartz–tremolite–calcite equilibria). The calculated values of fH_2O in the different rock types are consistent with buffering of fluid composition by mineral reactions. These data place constraints on the volume of the fluid reservoir during metamorphism as well as on the degree of communication of metamorphic fluids in the different rock types (*e.g.*, Ferry, 1978).

Appendix: activity–composition relations for crystalline solutions

Some of the activity–composition relations for crystalline solutions have been discussed in the text of this paper; others are discussed below.

Quartz was considered to be pure SiO_2. Electron microprobe analyses of kyanite and sphene indicate very small amounts of solid solution, and these phases were considered to be pure Al_2SiO_5 and Ca $TiSiO_5$, respectively.

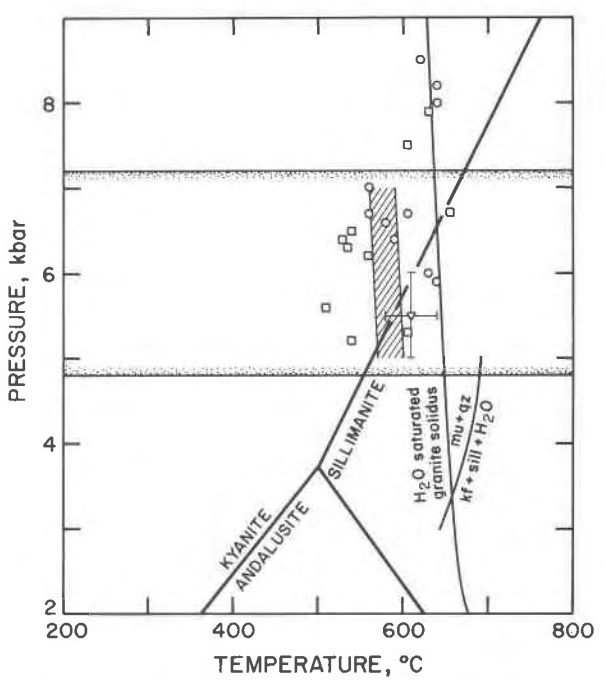

Fig. 4. Pressure–temperature diagram summarizing results of this paper. Circles: garnet–biotite T (Thompson calibration) and P from reaction 8; squares: garnet–biotite T (Goldman and Albee equation 6) and P from reaction 8; inverted triangle: T from GM75-4 and GM77-10 showing P and T limits; steep panel with hachure: calcite–dolomite temperatures; horizontal lines with stippling: approximate limits on bathozone 5 of Carmichael (1978). Aluminum silicate diagram from Holdaway (1971), muscovite + quartz stability from Chatterjee and Johannes (1974), granite solidus from Piwinskii (1968) and Boettcher and Wyllie (1968).

The tremolite activity in amphibole is treated as an ideal solution, and $a_{tr}^{Ca\,amph} = [3 - Ca - Na - K]\cdot[Ca/2]^2\cdot[Mg/5]^5\cdot[OH/2]^2$, where $[3 - Ca - Na - K]$ is the number of atoms on the A site, $[Ca/2]$ is the mole fraction of Ca on 2 M_4 sites, $[Mg/5]$ is the mole fraction of Mg in the M_1, M_2, and M_3 sites, and $[OH/2]$ is the mole fraction of hydroxyl in two anionic sites (Skippen and Carmichael, 1977).

For the activity of zoisite in epidote, $a_{zo}^{ep} = [Ca/2]^2\cdot[1 - (Fe+Mn+Ti)]\cdot[Si/3]^3\cdot[OH]$, where $[Ca/2]$ is the mole fraction of Ca in two divalent cation sites, $[1 - (Fe + Mn + Ti)]$ is the mole fraction of Al on one octahedral site, $[Si/3]$ is the mole fraction of Si on 3 tetrahedral sites and $[OH]$ is the mole fraction of hydroxyl on one anionic site (Skippen and Carmichael, 1977). Cation ordering on octahedral sites is assumed.

For the activity of phlogopite in biotite, $a_{phl}^{bi} = [K]\cdot[Mg/3]^3\cdot[OH/2]^2$, where $[K]$ is the mole fraction of K in the A sites, $[Mg/3]$ is the mole fraction of Mg on 3 M sites, and $[OH/2]$ is the number of hydroxyl ions on 2 anionic sites (Skippen and Carmichael, 1977; see also Kerrick and Darken, 1975).

The activity of diopside in clinopyroxene is calculated from

$$a_{di}^{cpx} = \frac{[Ca]\cdot(Mg)\cdot(Fe + Mg + Ca + Na - 1)}{(Fe + Mg)}\cdot[Si/2]^2$$

where $[Ca]$ is the mole fraction of Ca on M_2, (Mg) is the total number of Mg atoms, $(Fe + Mg + Ca + Na - 1)$ is the total Fe + Mg + Ca + Na atoms minus one and $(Fe + Mg)$ is the total number of Fe plus Mg atoms. The term $(Mg)\cdot(Fe + Mg + Ca + Na - 1)$ is the mole fraction of Mg on M_1. Because of the low Al content, the tetrahedral sites are considered to be completely filled by Si. Details of the solution model are discussed by Nicholls (1977, p. 128–129).

For staurolite, the formula used is $HFe_2Al_9Si_4O_{24}$, and because of the low minor-element content Mg–Fe substitution is considered to take place on the 2 four-fold sites occupied by Fe in end-member staurolite (see Griffen and Ribbe, 1973, p. 492 for discussion). This yields $a_{Fe\ st}^{st} = (XFe)^2$ where XFe is the mole fraction of Fe on the tetrahedral sites. Using a different ideal solution model for staurolite would not substantially change the conclusions that fH_2O estimated from staurolite–quartz–garnet–kyanite equilibria are much lower than those estimated from paragonite–quartz–albite–kyanite equilibria.

Acknowledgments

We thank John Ferry for a very constructive review. Robert Fudali and Ian Hutcheon also made constructive comments. Any remaining opacity or errors are our responsibility. We thank Philip Simony for his help at various stages of the project. B. Rutherford, R. Irish, L. Fisk, K. Siemens, and D. Worsick assisted with the collection, processing, and reporting of the data. We acknowledge financial support from National Research Council of Canada Operating Grant A-4379 (to Ghent) and Geological Survey of Canada EMR Research Agreement 1135-D13-4-83-73 (to Ghent and Simony).

References

Bickle, M. J. and R. Powell (1977) Calcite–dolomite geothermometry for iron-bearing carbonates. *Contrib. Mineral Petrol., 59,* 281–292.

Blümel, P. and W. Schreyer (1977) Phase relations in pelitic and psammitic gneisses of the sillimanite–potash feldspar and cordierite–potash feldspar zones in the Moldanubicum of the Lam-Bodenmais area, Bavaria. *J. Petrol., 18,* 431–459.

Boettcher, A. L. (1970) The system $CaO–Al_2O_3–SiO_2–H_2O$ at high pressures and temperatures. *J. Petrol., 11,* 337–379.

——— and P. J. Wyllie (1968) Melting of granite with excess water to 30 kilobars pressure. *J. Geol., 76,* 235–244.

Burnham, C. W., J. R. Holloway and N. F. Davis (1969) Thermodynamic properties of water to 1000°C and 10,000 bars. *Geol. Soc. Am. Spec. Pap., 132.*

Carmichael, D. M. (1978) Metamorphic bathozones and bathograds: a measure of the depth of post-metamorphic uplift and erosion on the regional scale. *Am. J. Sci., 278,* 769–797.

Chatterjee, N. D. (1972) The upper stability limit of the assemblage paragonite and quartz and its natural occurrences. *Contrib. Mineral. Petrol., 48,* 89–114.

——— (1976) Margarite stability and compatibility relations in the system $CaO–Al_2O_3–SiO_2–H_2O$ as a pressure–temperature indicator. *Am. Mineral., 61,* 699–709.

——— and W. Johannes (1974) Thermal stability and standard thermodynamic properties of synthetic 2M muscovite, $KAl_2[AlSi_3O_{10}(OH)_2]$. *Contrib. Mineral Petrol., 48,* 89–114.

Eugster, H. P., A. L. Albee, A. E. Bence, J. B. Thompson, Jr. and D. R. Waldbaum (1972) The two-phase region and excess mixing properties of paragonite–muscovite crystalline solutions. *J. Petrol., 13,* 147–179.

Ferry, J. M. (1976) *P*, *T*, f_{CO_2} and f_{H_2O} during metamorphism of calcareous sediments in the Waterville–Vassalboro area, south-central Maine. *Contrib. Mineral. Petrol., 57,* 119–143.

——— (1978) What do mapped isograds tell us about regional patterns of heat transfer and fluid flow during metamorphism? (abstr.) *Geol. Soc. Am. Abstracts with Programs, 10,* 400.

——— and F. S. Spear (1978) Experimental calibration of the partitioning of Fe and Mg between biotite and garnet. *Contrib. Mineral. Petrol., 66,* 113–117.

Ganguly, J. (1972) Staurolite stability and related parageneses: theory, experiments and applications. *J. Petrol., 13,* 335–365.

Ghent, E. D. (1975) Temperature, pressure and mixed volatile equilibria attending metamorphism of staurolite–kyanite bearing assemblages, Esplanade Range, British Columbia. *Geol. Soc. Am. Bull., 86,* 1654–1660.

——— (1976) Plagioclase–garnet–Al_2SiO_5–quartz: a potential geobarometer-geothermometer. *Am. Mineral., 61,* 710–714.

———, J. Nicholls, M. Z. Stout and B. Rottenfusser (1977a) Clinopyroxene amphibolite boudins from Three Valley Gap, British Columbia. *Can. Mineral., 15,* 269–282.

———, P. S. Simony, W. Mitchell, J. Perry, D. Robbins and J. Wagner (1977b) Structure and metamorphism in southeast Ca-

noe River area, British Columbia. *Rept. Activities Geol. Surv. Canada, Part C, Paper 77-1C,* 13–17.

Goldman, D. S. and A. L. Albee (1977) Correlation of Mg/Fe partitioning between garnet and biotite with O^{18}/O^{16} partitioning between quartz and magnetite. *Am. J. Sci., 277,* 750–761.

Goldsmith, J. R. and R. C. Newton (1969) *P–T–X* relations in the system $CaCO_3$–$MgCO_3$ at high temperatures and pressures. *Am. J. Sci., 267A,* 160–190.

Gordon, T. M. and H. J. Greenwood (1970) The reaction: dolomite + quartz + water = talc + calcite + carbon dioxide. *Am. J. Sci., 268,* 225–242.

Griffen, D. T. and P. Ribbe (1973) The crystal chemistry of staurolite. *Am. J. Sci., 273-A,* 479–495.

Hensen, B., R. Schmid and B. J. Wood (1975) Activity–composition relationships for pyrope–grossular garnet. *Contrib. Mineral. Petrol., 51,* 161–166.

Hewitt, D. S. (1975) Stability of the assemblage phlogopite–calcite–quartz. *Am. Mineral., 60,* 391–397.

Holdaway, M. J. (1971) Stability of andalusite and the aluminum silicate phase diagram. *Am. J. Sci., 271,* 97–131.

Holloway, J. R. (1977) Fugacity and acitivity of molecular species in supercritical fluids. In D. G. Fraser, Ed., *Thermodynamics in Geology,* p. 161–181. Reidel, Dordrecht, Holland.

Hoschek G. (1973) Die Reaktion Phlogopit + Calcit + Quarz = Tremolit + Kalifeldspat + H_2O + CO_2. *Contrib. Mineral. Petrol., 39,* 231–237.

Hunt, J. A. and D. M. Kerrick (1977) The stability of sphene: experimental redetermination and geologic implications. *Geochim. Cosmochim. Acta, 41,* 279–288.

Kerrick, D. M. and L. S. Darken (1975) Statistical thermodynamic models for ideal oxide and silicate solid solutions, with applications to plagioclase. *Geochim. Cosmochim. Acta, 39,* 1431–1442.

Newton, R. C. (1966) Some calc-silicate equilibrium relations. *Am. J. Sci., 264,* 204–222.

———, T. V. Charlu and O. J. Kleppa (1977) Thermochemistry of high pressure garnets and clinopyroxenes in the system CaO–MgO–Al_2O_3–SiO_2. *Geochim. Cosmochim. Acta, 41,* 369–377.

Nicholls, J. (1977) The calculation of mineral compositions and modes of olivine–two pyroxene–spinel assemblages. *Contrib. Mineral. Petrol., 60,* 119–142.

Orville, P. M. (1972) Plagioclase cation exchange equilibria with aqueous chloride solution: results at 700°C and 2000 bars in the presence of quartz. *Am. J. Sci., 272,* 234–272.

——— (1974) The "peristerite gap" as an equilibrium between ordered albite and disordered plagioclase solid solution. *Bull. Soc. fr. Mineral. Cristallogr., 97,* 386–392.

Pigage, L. C. (1976) Metamorphism of the Settler Schist. *Can. J. Earth Sci., 13,* 405–421.

Piwinskii, A. J. (1968) Experimental studies of igneous rock series, central Sierra Nevada batholith, California. *J. Geol., 76,* 548–570.

Puhan, D. (1978) Experimental study of the reaction: dolomite + K-feldspar-phlogopite + calcite + CO_2 at the total gas pressures of 4000 and 6000 bars. *Neues Jahrb. Mineral. Monatsh.,* 110–127.

——— and W. Johannes (1974) Experimentelle Untersuchung der Reaktion Dolomit + Kalifeldspat + H_2O = Phlogopit + Calcit + Quarz. *Contrib. Mineral. Petrol., 48,* 23–31.

Rice, J. M. (1977) Contact metamorphism of impure dolomitic limestone in the Boulder Aureole, Montana. *Contrib. Mineral. Petrol., 59,* 237–259.

Richardson, S. W. (1968) Staurolite stability in part of the system Fe–Al–Si–O–H. *J. Petrol., 9,* 757–768.

Robie, R. A. and D. R. Waldbaum (1968) Thermodynamic properties of minerals and related substances at 298.15 K (25°) and one atmosphere (1.013 bars) pressure and at higher temperatures. *U.S. Geol. Surv. Bull. 1259.*

Skippen, G. B. (1975) Thermodynamics of experimental sub-solidus silicate systems including mixed volatiles. *Fortschr. Mineral, 52,* 75–99.

——— and D. M. Carmichael (1977) Mixed-volatile equilibria. In H. J. Greenwood, Ed., *Short Course in Application of Thermodynamics to Petrology and Ore Deposits,* p. 109–125. Mineralogical Association of Canada Short Course Handbook 2.

——— and W. Yzerdraat (1970) XCDFOR: a Fortran IV program for calculating equilibria on T–XCO_2 sections. *Carleton Univ. Geol. Pap. 1970-3,* Ottawa.

Smith, J. V. (1968) The crystal structure of staurolite. *Am. Mineral., 53,* 1139–1155.

Thompson, A. B. (1975a) Mineral reactions in a calc-mica schist from Gassetts, Vermont, U.S.A. *Contrib. Mineral. Petrol., 53,* 105–127.

——— (1975b) Calc-silicate diffusion zones between marble and pelitic schist. *J. Petrol., 16,* 314–346.

——— (1976) Mineral reactions in pelitic rocks: II. Calculation of some *P–T–X* (Fe–Mg) phase relations. *Am. J. Sci., 276,* 401–454.

Thompson, J. B., Jr. (1967) Thermodynamic properties of simple solutions. In P. H. Abelson, Ed., *Researches in Geochemistry, 2,* p. 340–361. Wiley, New York.

Tracy, R. J., P. Robinson and A. B. Thompson (1976) Garnet composition and zoning in the determination of temperature and pressure of metamorphism, central Massachusetts. *Am. Mineral., 61,* 762–775.

Velde, B. (1965) Phengite micas: synthesis, stability, and natural occurrence. *Am. J. Sci., 263,* 886–913.

Vidale, R. J. and D. A. Hewitt (1973) "Mobile" components in the formation of calc-silicate bands. *Am. Mineral., 58,* 991–997.

Wise, W. S. and H. P. Eugster (1964) Celadonite: synthesis, thermal stability, and occurrence. *Am. Mineral, 49,* 1031–1083.

Woodsworth, G. J. (1977) Homogenization of zoned garnets from pelitic schists. *Can. Mineral., 15,* 230–242.

Manuscript received, July 31, 1978;
accepted for publication, December 14, 1978.